Characterization of MAST neutron camera detectors and first measurements

S. Sangaroon[1], M. Cecconello[1], I. Wodniak[1], C. Marini Bettolo[1], M. Turnyanskiy[2], G. Ericsson[1], and MAST team[2]
[1] *Department of Physics and Astronomy, Uppsala University, Uppsala, Sweden (EURATOM-VR Association)*
[2] *EURATOM/CCFE Fusion Association, Culham Science Centre, Abingdon, United Kingdom*

1. Introduction and instrument description

At MAST, 2.45 MeV neutrons are produced by the beam thermal D-D fusion reactions which occur in neutral beam heated discharges and measured with the neutron camera (NC) system described in [1]. The neutron emissivity profile carries important information on the physics of fast particles and of plasma instabilities and is measured by the NC which is equipped with two equatorial and two diagonal collimated lines of sight (LoS). The NC's four LoS are now all installed and its commissioning has been completed. The detectors consist of $2 \times 5 \times 1$ cm^3 EJ-301 liquid scintillators coupled to Hamamatsu R5611 photomultiplier tubes (PMT). The detectors' characterization is necessary not only to compare different plasma scenarios with different neutron yields but also to compare the NC measurements with, for example, fission chamber's (FC) measurements. A 5 kHz light emitting diode (LED) provides a square light pulse 100 ns wide which is fed via a fiber bundle to all four scintillators and can be used for monitoring the stability of the PMTs. Each detector is equipped with a ^{22}Na source which is used for energy calibration. PMTs are well known to be very sensitive to magnetic fields and, although they are enclosed by a double soft iron box with a μ-metal layer, a 3-axis magnetic field sensor has been installed for monitoring purposes. In addition, each detector is equipped with a temperature sensor to avoid overheating the scintillators.

2. Detector characterization

The characterization of the detectors consists of: i) detectors' energy resolution and response function for gamma rays; ii) pulse shape discrimination capabilities and its dependence on temperature; iii) PMT gain variations with temperature, magnetic field, count rate and applied high voltage. The energy resolution of liquid scintillators is based on the determination of the position in a pulse height spectrum of the Compton maximum, half-maximum and edge. For the MAST NC detectors the position of the Compton edge has been determined to be at 0.89847 of the Compton edge maximum by using a simulated recoil electron pulse height spectrum, obtained via a MCNP simulation, folded with the detector resolution function

assumed to be the normal distribution with different resolutions, from 5 to 35 %. The knowledge of the Compton edge position permits the energy calibration of the pulse height spectrum (done using ^{137}Cs and ^{22}Na gamma sources) from which the detector energy resolution can be measured. The energy resolution dependence on the gamma energy is shown in figure 1: the results are in agreement with those found in literature and can be modelled by the light output function $\Delta L/L = [\alpha^2 + \beta^2/L + \gamma^2/L^2]^{1/2}$. The parameters α, β and γ are obtained by a non-linear least square fit of the MCNP simulated PHS folded with the resolution function to the measured PHS in the energy region 0.10 - 1.15 MeV. The result of this fit, shown in figure 2, gives $\alpha = 16.47 \pm 1.06$, $\beta = 16.19 \pm 0.58$ and $\gamma = 4.03 \pm 0.41$ with a $\chi^2_{red} = 1.24$. The resolution function calculated using α, β and γ so obtained is compared to the experimentally measured resolution as show in figure 1.

The pulse shape discrimination capability of the detectors has been studied using a ^{252}Cf source which emits both neutrons and gammas: the figure of merit (gamma and neutron peaks separation divided by the sum of the peaks' FWHM) at room temperature is 0.81 and it increases by 7.78% over the temperature range 20°C to 30°C. The PMT gain variations due to temperature changes are negligible, however variations due to magnetic field and count rate are not. A maximum magnetic field of 0.34 mT at the detector position was measured in an ohmic pulse, with a partially closed magnetic shielding, during which the gain of the PMT dropped by 13.32 % as show in figure 3. The PMT gain stability as a function of count rate and applied voltage has been carried out and the results are shown in figure 4: this gain variation was calculated using the LED pulses which also provide the compensation factor.

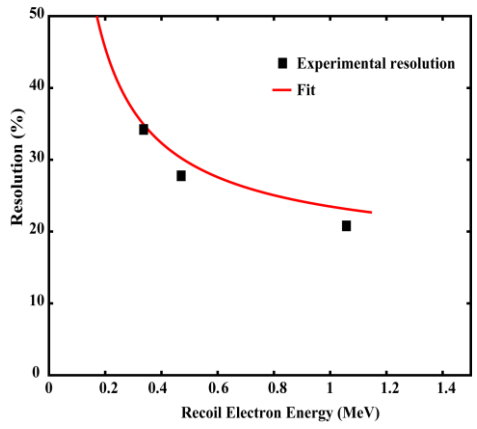

Figure 1. Pulse height resolution function $\Delta L/L$ (in %) dependence on recoil electron energy.

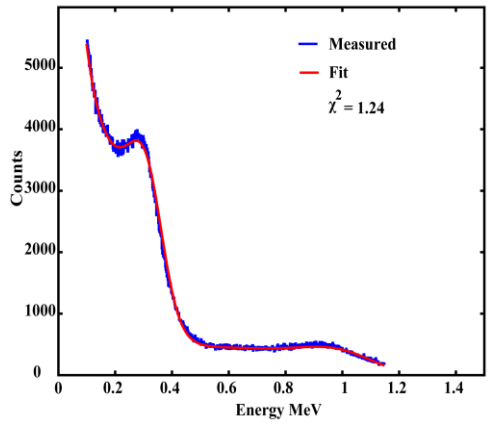

Figure 2. Comparison between experimental and simulated PHS for the recoil electron.

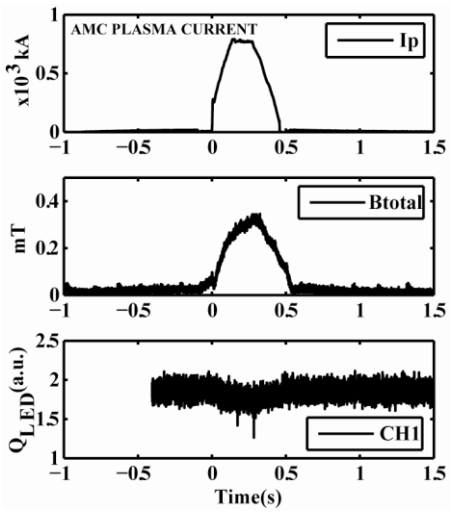

Figure 3. PMT gain variation due to stray magnetic field as measured at the detector location.

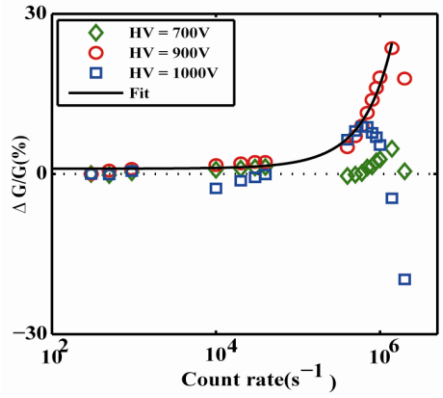

Figure 4. An example of gain variation with different count rate and voltage supply of detector SEK470.

At count rates larger than 5×10^5 s^{-1} the gain depends not only on the count rate but also on the applied voltage too.

3. Experimental results and conclusions

Initial results from the completed NC are discussed for pulse 26086 which is characterized by a high NBI power between 0.041 – 0.325 s: global plasma parameters together with the total count rate for the four channels are illustrated in figure 5. The plasma current is 0.2-0.7 MA, the line integrated electron density is $0.01\text{-}1.69 \times 10^{20}$ m^{-2}, the NBI power 1.2-3.2 MW. The neutron yield rate from FC had a maximum yield rate of $Y_n \approx 7.26 \times 10^{13}$ s^{-1}. The total count rates observed for the NC are as high as 1.32×10^6 s^{-1}. At such high count rates PMT gain variations are expected as indeed observed as shown in figure 4. The results indicate that the PMT gain variation depends not only on the count rate but also on the shape of the signals: the amplitude of the LED pulses increased up to 43.53% while γ and neutron pulse amplitudes decreased by 41.21% due to count rate higher than 5×10^5 s^{-1} as shown in last two panels of figure 5. At such high count rates, pile-up is also occurring requiring a more sophisticated PSD analysis. The effect of pile-up is visible in figure 6 (top left) as points outside the expected neutron, gammas and LED regions. In this study 44% of the pulses are polluted by pile-up and discarded. The results show clearly n/γ distribution in bottom left panel, figure 6. The LED pulses were extracted to observe the gain variation due to count rate as show in last panel of figure 5. The γ rays distribution is in the red area, while neutrons are visible in the blue area in bottom right panel of figure 6. The preliminary analysis of neutron yield of NC with FC is in figure 7, top panel. The neutron yield observed for the NC is as high as 4.66×10^5 s^{-1} while γ rays are 2.92×10^5 s^{-1}. Each data point shown in the bottom panel of figure 7 represents the count rate of NC and FC over the NBI period. The results show a non-linear dependence between the NC and FC count rates for NC neutron yield above

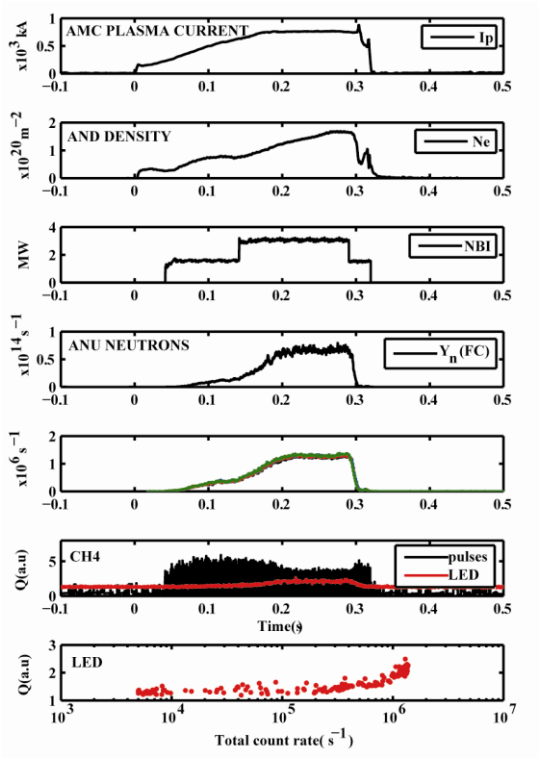

Figure 5. Time traces of plasma parameters for MAST pulse 26086, Ip, Ne, NBI, neutron yield as measured by the FC, total count rates measured by the four channels of the NC, and the gain variation due to count rate during NBI period.

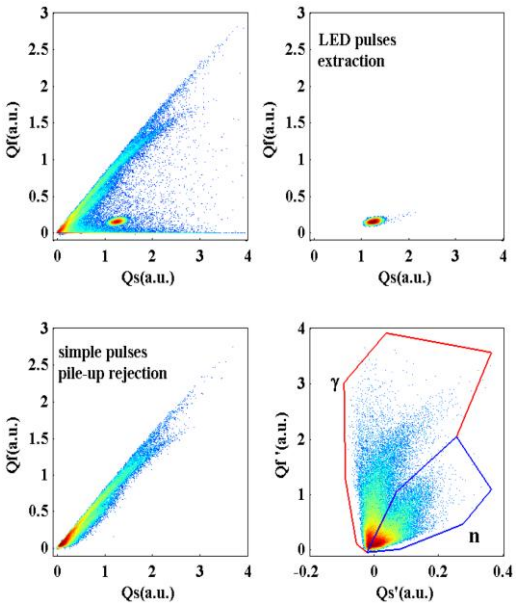

Figure 6. Top left: the distribution in Q_f-Q_s of all pulses. Top right: the LED extraction. The n/γ distributions with simple pile-up rejection are in the bottom panels.

1.10×10^5 s^{-1} due to pile-up rejection. The neutron count rate corrected for pile-up rejection is shown in figure 7. The correction is obtained by adding $F_n P_{CR}$ to the neutron count rate where P_{CR} is the total (γ + n) pile-up rejection count rate and F_n is equal to the ratio of the neutron count rate to the sum of the neutron and γ count rates. The NC is now ready for the next MAST experiment campaign although some improvements are still required in the gain compensation and pile-up rejection.

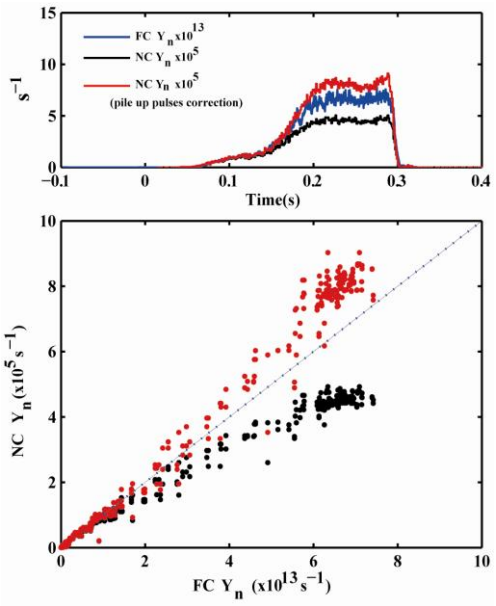

Figure 7. Top panel: neutron yield comparison between NC and FC with (red) and without (black) the correction for pile-up rejection. Bottom panel: NC yield versus FC yield.

4. Reference

[1] M. Cecconello et al, *Rev. Sci. Instrum.* 81, 10D315 (2010)

Acknowledgments

This work was funded jointly by the United Kingdom Engineering and Physical Sciences Research Council and by the European Communities under the contract of Association between EURATOM and CCFE, and by the Swedish Research Council and by the European Communities under the contract of Association between EURATOM and VR. The views and opinions expressed herein do not necessarily reflect those of the European Commission.